Aspergillus nidulans hypA regulates morphogenesis through the secretion pathway[☆]

Xianzong Shi,[1] Yu Sha,[2] and Susan Kaminskyj[*]

Department of Biology, University of Saskatchewan, Saskatoon, SK, Canada S7N 5E2

Abstract

Aspergillus nidulans hypA encodes a predicted 1474 amino acid, 161.9 kDa cytoplasmic peptide. Strains with *hypA1* and *hypA6* alleles are wild type at 28 °C but have wide, slow-growing hyphae and thick walls at 42 °C. *hypA1* and *hypA6* have identical genetic lesions. *hypA1* and *hypA6* restrictive phenotypes have statistically similar morphometry, and strains with either allele can conidiate at 42 °C. *hypA* deletion strains require osmotic support and have aberrant morphology, but produce viable spores at 28 °C. *hypA* has full-length orthologs in filamentous fungi and yeasts and a 200 amino acid region with similarity to sequences in plants and animals. The *Saccharomyces cerevisiae hypA* ortholog is *TRS120*, a regulatory subunit in the TRAPP II complex that mediates traffic through the Golgi equivalent. Enzyme secretion is reduced in *hypA1* cells at 42 °C. Endomembranes and cytoplasmic actin arrays in *hypA1* have weak polarity at 42 °C and cytoplasmic microtubules have reduced number and normal distribution.
© 2003 Elsevier Inc. All rights reserved.

Keywords: Filamentous fungi; *Aspergillus nidulans*; Morphogenesis; Secretion; Endomembranes; Cytoskeleton; *hypA*

1. Introduction

The elegant tubular forms of fungal hyphae are produced by polarized cell extension called tip growth. Hyphae grow by inserting wall-building vesicles at the tip, so that altering the position and/or rate of vesicle insertion affects hyphal shape. Hyphal morphogenesis simulated using a mathematical model based on a "vesicle supply center" from which wall-building vesicles are directed to the cell surface (Bartnicki-Garcia, 1990, 2003) produces hyphal profiles that closely resemble those in micrographs. The theoretical position of this supply center is coincident with the Spitzenkörper, an apical assemblage of vesicles and cytoskeletal elements whose dynamics predict growth direction and shape of fungal hyphae (Bartnicki-Garcia et al., 1995; Lopez-Franco et al., 1994). Nevertheless, the role of the Spitzenkörper is unclear, as tip growth is also seen in *Neurospora crassa* (Seiler et al., 1997) and *Nectria haematococca* (Wu et al., 1998) kinesin-deletion mutants which lack or have aberrant Spitzenkörper, respectively; in oomycetes like *Saprolegnia ferax* which lack Spitzenkörper but have an analogous structure (Jackson and Heath, 1990b); and in tip-growing plant and algal cells whose tip architecture is different yet again (e.g., Miller et al., 1996).

Major structural components of fungal hyphae include the cell wall, which maintains mature cell shape externally (Gooday, 1994) and actin arrays that provide internal reinforcement at the growing tip (Jackson and Heath, 1990a). In fungi including *Aspergillus nidulans*, the wall contains chitin fibrils produced by a family of chitin synthases (Borgia and Dodge, 1992; Motoyama et al., 1994, 1997; Munro et al., 1998). Single chitin synthase deletions have little effect on hyphal morphogenesis, so many of these genes appear to have overlapping

[*] Corresponding author. Fax: +306-966-4461.
E-mail addresses: Xianzong.Shi@usask.ca (X. Shi), yus661@duke.usask.ca (Y. Sha), Susan.Kaminskyj@usask.ca (S. Kaminskyj).
[1] Present address: Department of Biochemistry, University of Saskatchewan, 105 Wiggins Ave, Saskatoon, SK, Canada S7N 5E5.
[2] Present address: Department of Microbiology, University of Saskatchewan, 107 Wiggins Ave, Saskatoon, SK, Canada S7N 5E5.

functions. However, an *A. nidulans* Δ*chsA*, Δ*chsC* double mutant had reduced hyphal wall integrity (Ichinomiya et al., 2002a; Makoto et al., 2000) and *chsB* has been implicated in normal hyphal growth (Ichinomiya et al., 2002b).

The cytoplasm produces and transports to the tip the exocytic vesicles that contain cell wall matrix and fibril synthetic complexes. Cytoskeletal filaments also provide internal support at sites of cell extension (Heath, 1990; Jackson and Heath, 1990a; Kaminskyj and Heath, 1996). In *A. nidulans*, actin is associated with tip growth (Harris et al., 1994), along with myosin (McGoldrick et al., 1995), and other presumably actin binding proteins. Harris et al. (1994) and Momany and Hamer (1997) have shown that actin is required for septation in *A. nidulans*. In addition, actin microfilaments and cytoplasmic microtubules are important for Spitzenkörper stability (Riquelme et al., 1998), and septins, a type of intermediate filament, are essential for polarization and septation (Westfall and Momany, 2002).

Regulatory components of hyphal morphogenesis include cytoplasmic ions, notably calcium (e.g., Jackson and Heath, 1993; Dayton and Means, 1996), hydrogen (Bachewich and Heath, 1997), and manganese (Sone and Griffiths, 1999), as well as second messengers like cAMP (Bruno et al., 1996; Adachi and Hamer, 1998), *ras* gene function (Som and Kolaparthi, 1994), and components of the endomembrane system (Whittaker et al., 1999). Hyphal morphology can vary within the life cycle of a single species, especially during pathogenesis and often modulated by the factors discussed above (e.g., Adachi and Hamer, 1998; Gale et al., 1998; Mayorga and Gold, 1999; Shi et al., 1998). Nevertheless, the list of morphogenetic factors identified so far is undoubtedly incomplete. As in many fungi, screens to identify additional hyphal morphogenesis genes in *A. nidulans* are ongoing (Harris et al., 1999; Kaminskyj and Hamer, 1998; Momany et al., 1999; Osherov et al., 2000).

Kaminskyj and Hamer (1998) identified five morphogenesis loci (*hypA*–*hypE*) by screening a temperature-sensitive mutant collection. <u>hyp</u>ercellular strains have aberrant, nonlethal morphogenesis defects at restrictive temperature. Analysis of the *hypA1* phenotype suggests that wild-type *hypA* promotes tip growth and restrains growth of basal cells (Kaminskyj, 2000; Kaminskyj and Hamer, 1998; Momany et al., 1999). Here, we show that *hypA* is a nonessential gene involved in the secretion pathway, compare two *hypA* conditional alleles, and show the endomembrane and cytoskeletal consequences of *hypA* defects in living cells.

2. Materials and methods

The biological materials and primers used in this study are listed in Table 1. Unless specified otherwise,

reagents were supplied by Sigma (www.sigma-aldrich.com) or VWR (www.vwrcanlab.com). All water was Type I (18 MΩ resistant) and autoclaved or RNase free as needed. *A. nidulans* strains were grown as described in Kaminskyj (2001) and Kafer (1977) and nutritionally supplemented as needed. An *A. nidulans* strain containing GFP (green fluorescent protein)-tagged α-tubulin under the control of an *alcA* promoter (a gift of N.R. Morris and X. Xiang) was mated to *hypA1* and *hypA6* strains (Kaminskyj, 2001) to create strains with GFP-tagged microtubules. *Escherichia coli* strains were grown and plasmid DNA was manipulated as described in Sambrook et al. (1989).

Like other true fungi, but unlike oomycete fungi, animals, and plants, *A. nidulans* does not have a classical Golgi body consisting of stacked cisternae. Instead, it has single pleiomorphic cisternae called dictyosomes or Golgi equivalents that appear to have similar function. Since most of the *hypA*-related research has been in *Saccharomyces cerevisiae*, where the term Golgi is commonly used, we will use the term Golgi equivalent.

2.1. Cloning and molecular analysis

Transformation followed the method of Osmani et al. (1987), using germlings protoplasted with Driselase (Interspex, www.wenet.net/~sharma/interspex), Glucanex (Interspex), and β-glucuronidase, and about 10^8 protoplasts in a final volume of 1200 µl transformation mix. Protoplasts were cotransformed with cosmid (Brody et al., 1991), plasmid, or restriction fragment DNA, plus 1 µg ARp1 DNA (Gems et al., 1991) that contains *N. crassa pyr4$^+$* as a selectable marker. After transformation, aliquots of protoplast suspension were mixed with MM or CM (lacking the selection marker) containing 0.6% agar and 1 M sucrose and plated over the same medium containing 1.5% agar. Protoplasts were incubated at 28 °C for 24 h before testing for phenotype complementation at 42 °C.

For *hypA* deletion, the *argB* deletion strains A850, A851, or A852 were transformed with 10 µg pΔ*hypA*::*argB* (described below) after digestion with *Xba*I and *Kpn*I to release the deletion cassette. Transformants were grown at 28 °C and selected for arginine prototrophy. Δ*hypA*::*argB* strains were grown on MM agar containing 1 M sucrose as osmoticum. The cassette for replacing *hypA* with *argB*, pΔ*hypA*::*argB*, was made by ligating a *Bam*HI digest containing the coding region of *A. nidulans* ornithine decarboxylase (*argB*) with PCR-amplified orthologous arms from genomic sequences immediately upstream and downstream of *hypA*, and cloning into pBluescript II SK$^+$ (Stratagene, www.stratagene.com). PCR amplification of the arms was done in 100 µl PCRs containing 1× TNK50 buffer (Blanchard et al., 1993), 0.1 mM each dNTP, 0.2 µM each primer, 2.5 U *Taq* DNA polymerase (Promega,

Table 1
Biological materials used in this study

Aspergillus nidulans strains	
A28[a]	*biA1, pabaA6; veA1*
A850[a]	*biA1; ΔargB:: trpCΔB; methG1; veA1 trpC801*
A851[a]	*pabaA1 yA2; ΔargB:: trpCΔB; veA1 trpC801*
A852[a]	*biA1; ΔargB:: trpCΔB; methG1; veA1 trpC801/pabaA1 yA2; ΔargB::trpCΔB; veA1 trpC801*
ASH80[b]	*hypA6, biA1, pabaA6; veA1*
ASK30[c]	*hypA1; wA2; pyroA4; veA1*
ASK37[d]	*pyrG89 hypA1 biA1 pabaA6; wA2; veA1*
AYS2[d]	*hypA6; wA2; veA1; alcA*: GFP α-tubulin
AYS3[d]	*hypA1; wA2; veA1; alcA*: GFP α-tubulin
Cosmids	
SL22E6[a],[e]	*A. nidulans* chromosome IR, kan^R
C6G9[e]	*Schizosaccharomyces pombe*, CAB11291, kan^R
SC70914[g]	*Saccharomyces cerevisiae*, TRS120NP_0.0695.1, amp^R
NC96412[a]	*Neurospora crassa*, TREMBL: AF149719_1, kan^R
NC6B5[a]	*Neurospora crassa*, TREMBL: AF149719_1, kan^R
Plasmids	
ARp1[h]	Autonomously replicating plasmid, *pyr4* marker, amp^R
pSal*argB*[i]	1.8 kb *Bam*HI fragment containing *argB* in pUC18, amp^R
pSKJ1[d]	upstream region and 5′ end of *hypA*, in pBluescript SK+, amp^R
pSKJ22[d]	3′ end and downstream region of *hypA* in pBluescript SK+, amp^R
pΔ*hypA::argB*[d]	See Fig. 2 and Materials and Methods; in pBluescript SK+, amp^R
Primers	Sequence 5′ → 3′
P1Sac[j]	ACGGAGCTCACCGGCGATAC
P2Bam[j]	CCGGATCCTTGCTGCCGATGCCTTAGA
P9Xba[j]	G CCTCTAGAGGAGCGACACCATAGCGTA
P10Bam[j]	CCGGATCCATCGTGACACCGAATG
P12Kpn[j]	CCGGTACCAATCTGGGAGCGCTTCACA
P13Bam[j]	CCGGATCCGGACACGTACCGTCTAAC
P14Kpn[j]	CCGGTACCCCAGTACGGACAGC
3C1[k]	AGAGGCCTGTTCGTCGATsC
3C2[k]	TCACTGCGACGAGTGAGAAsG
5B1[k]	GTACCAGTGCCCTTGGATTsC
5B2[k]	CGGCTTCGATGGCTTGTsC
5C1[k]	GCCCTCTTCTTGTGCGATAsC
5C2[k]	GGTACACCCTCGCTCTCAAsG
5C3[k]	GGTGGTGCTGGACCGACTAsG
5C4[k]	TCAGGATCCGGCGAACTTTsG
PA3-T$_{18}$V[k]	GGGGTACCTCAGACGGACTAT$_{18}$V
PA5[k]	GCTCTAGAGCGGTGAGCATGA
PargB1[j]	CTGCTGGCGGACTTATGAG
PargB2[j]	GGAATGATCTCATACCCGTCA

[a] Fungal Genetics Stock Center, U Kansas (www.fgsc.net).
[b] a gift of Steven Harris, U Nebraska.
[c] Kaminskyj and Hamer, 1998.
[d] This study.
[e] Brody et al., 1991 (available from www.fgsc.net).
[f] A gift of the Sanger Centre (www.sanger.ac.uk/Projects/S_pombe/).
[g] American Type Culture Collection (www.atcc.org/atcc.html).
[h] Gems et al., 1991.
[i] K. Miller, U Idaho.
[j] Synthesized by GIBCO/Lifetechnologies (www.lifetech.com).
[k] 3′ base attached with a phosphorothioate linkage to prevent primer degradation by proofreading DNA polymerases. Synthesized by Cortec (www.cortec.queensu.ca/).

www.promega.com), and 100 ng L22E6 template. To increase cloning efficiency, 400 μl of each PCR was treated at 50 °C for 1 h with 50–100 μg/ml proteinase K (PCR grade, Roche Molecular Biochemicals, bio-chem.roche.com; Wybranietz and Lauer, 1998). PCR products were digested with *Bam*HI and *Xba*I or *Kpn*I, gel purified, and recovered by GeneClean II (Bio/Can Scientific, www.biocan.com) or the Concert Rapid Gel Extraction System (Gibco/Life Technologies), and ligated into pBluescript SK$^+$. The *Bam*HI fragment

containing *argB* was inserted using standard methods (Sambrook et al., 1989).

The *hypA* genomic region was sequenced using restriction enzyme-mediated subcloning (Sambrook et al., 1989) and transposon-mediated insertional mutagenesis (Strathmann et al., 1991). For the latter, XL1Blue strains containing either pSKJ1 or pSKJ22 (both amp^R) and DH5α-rif^R (a spontaneous mutant) were mated and plated on LB containing ampicillin (or methicillin) and rifampicin. Cells in which pSKJ1 or pSKJ22 had an insertion of the Tn1000 transposon (γδ class, activated by mating) were picked for insertion site determination using PCR with T3/GDIR and T7/GDIR primer pairs. Amplification used 25 cycles of 30 s denaturing at 94 °C, 60 s annealing at 60 °C, and 60 s extension at 72 °C. Reactions contained TNK50 buffer (Blanchard et al., 1993), 2.5 mM dNTPs each, 0.1 μM GDIR, and T3 (or T7) each, 2.5 U *Taq* DNA polymerase. Sequencing (DNA Sequencing Laboratory, NRC Plant Biotechnology Institute; U Saskatchewan Biology Organismal Genomics Research Lab) used primers GD1 and GD2. DNA sequence assembly used Sequencher 3.1.1 (Gene Codes Corporation, www.genecodes.com). Sequence analysis used DNAsis V2.0 (Hitachi Software Engineering, www.hitachi-soft.com), BLAST (Altschul et al., 1990: www.ncbi.nlm.nih.gov/BLAST/) and internet software tools.

To identify and compare the *hypA1* and *hypA6* lesions, ASK30, ASH80, and A28 genomic DNA was amplified by PCR using *Taq* polymerase, sequenced, and aligned with the wild-type *hypA* (GenBank AF001273). For each strain, at least three independent amplifications were used for each part of the *hypA* sequence, collectively spanning the entire gene, and both strands were sequenced for each base pair. *Pfx* DNA polymerase was not used because it can cause primer degradation, as discussed below. Lesion sites were confirmed using ASK37 and AYS1 protoplasts, cotransformed with 1 μg ARp1 and 2 μg amplicons (each about 1 kb) spanning the putative lesion sites from A28 genomic DNA, and selected at 42 °C.

The *hypA* cDNA was cloned by 3′- and 5′-RACE, as described in Shi and Kaminskyj (2000) and Shi et al. (2002). Rapid amplification of cDNA ends (RACE; Frohman et al., 1988) used Touchdown PCR (Don et al., 1991; Hecker and Roux, 1996). A 50 μl reaction contained 1.25 U (0.5 μl) Platinum *Pfx* DNA polymerase (GIBCO/Life Technologies, www.lifetech.com), 1× *Pfx* amplification buffer, 1 mM MgSO$_4$, 0.1 mM each dNTP, and 0.2 μM each primer. The primers for 3′-RACE were PA3-T$_{18}$V (V = A, C, G; Borson et al., 1992) and 3C1 or 3C2. Primers for 5′-RACE were PA5 and 5B1, 5B2 and 5C1–5C4 (Table 1). Primers used with *Pfx* were phosphorothioated to prevent degradation by proofreading activity (Skerra, 1992). The *hypA* cDNA sequence is GenBank AY251281.

2.2. Southern and Northern blot analysis

RNA and genomic DNA were prepared from about 10^9 *A. nidulans* spores germinated in 50 ml CM at 28 °C in a Gel Slick-treated flask shaken at 250 rpm for 16 h. Germlings were harvested by filtration, frozen in liquid nitrogen, and ground into powder at −80 °C. RNA was isolated using TriReagent (Molecular Research Center, www.mrcgene.com) and treated with DNase I. Messenger RNA was prepared using Oligotex Direct mRNA (Qiagen, www.qiagen.com). Genomic DNA was isolated as described by Yelton et al. (1984).

Ten micrograms of *Bam*HI-digested *A. nidulans* genomic DNA, or 50 μg total RNA or 3 μg mRNA were fractionated by agarose gel electrophoresis, and transferred to GeneScreen Plus (NEN Life Science, www.nenlifesci.com) in 20× SSPE. After UV crosslinking, nucleic acids were prehybridized (2–6 h) and then hybridized in 5× SSPE containing 5% SDS at 65 °C. Hybridization was overnight with the 1.8 kb *Sac*I fragment from pSKJ13 (Table 1) or with the pΔ*hypA*::*argB* insert that had been ^{32}P-labeled with an Oligolabelling Kit (Amersham Pharmacia Biotech, www.apbiotech.com). The hybridized blot was washed twice with excess 2× SSPE at room temperature, twice at 65 °C, and then with 0.5× SSPE + 0.1% SDS at 55 °C, if necessary. The signal was detected by exposing Bio-Max X-ray film (Eastman Kodak, www.kodak.com) at −80 °C with intensifier screens. Exposure times were overnight for the Southern blot and 4 days for the Northern blot.

2.3. Microscopy

Aspergillus nidulans strains were grown on coverslips in liquid medium (Kaminskyj, 2001), on dialysis tubing overlying agar, or directly on agar. Images were captured on Kodak TMax P3200 film, or with a Sensys digital camera (Roper Scientific, www.inovis.com) operated by MetaVue software (Universal Imaging, www.image1.com).

For immunofluorescence microscopy, A28 cells were grown on dialysis tubing at 28 °C and prepared following Kaminskyj and Heath (1994). To examine actin arrays in *hypA1* cells at 42 °C, spores were germinated in liquid shake culture overnight. Cells were permeabilized by freezing in liquid nitrogen (Raudaskoski et al., 1991) and thawing at room temperature. Actin arrays were localized using IC4 monoclonal anti-actin; cytoplasmic microtubules were localized using DM1A monoclonal anti-tubulin. Primary antibodies were visualized with FITC-conjugated rabbit anti mouse.

For FM4-64 staining of endomembranes, cells grown on agar were mounted in 25 μM FM4-64 in CM (Fischer-Parton et al., 2000) and imaged with a Zeiss META 510 laser scanning confocal microscope

For scanning electron microscopy, colonies grown at 42 °C for 5 days were fixed in OsO$_4$ vapor for 1 h at room temperature, frozen to −80 °C, dehydrated in −80 °C acetone, warmed stepwise to room temperature, lyophilized or critical point dried, gold coated in an Edwards S150B sputter coater, and examined with a JEOL 840A SEM. For transmission electron microscopy, *hypA1* cells were grown for 14 h or 5 d, then prepared following the method described in Kaminskyj (2000).

3. Results

The *hypA* locus was identified from a morphological screen of a temperature-sensitive *A. nidulans* mutant library. *hypA* has two temperature-sensitive alleles, *hypA1* (Kaminskyj and Hamer, 1998) and *hypA6*, identified independently as *podA1* (Harris et al., 1999) and *swoE1* (Momany et al., 1999) from the temperature-sensitive library described in Harris et al. (1994). At 42 °C both *hypA1* and *hypA6* strains grow slowly with aberrant morphology and thick walls. Previously, *podA1* was described as arresting after about 18 h at 42 °C, whereas *hypA1* was described as being able to complete its asexual life cycle at 42 °C. This disparity was due in part to the number of individuals sampled in the two studies. While most *hypA* temperature-sensitive germlings arrested in the first day, strains with either *hypA1* or *hypA6* can complete their asexual life cycle at 42 °C (Figs. 1A and B), and produce viable spores. These spores produce wild-type germlings at 28 °C and have the restrictive phenotype at 42 °C.

The fine structure of *hypA1* and *hypA6* strains grown at 42 °C was compared using transmission electron microscopy at 14 h and 5 days (Figs. 1C and D). At both ages the tip hyphal walls are at least fourfold thicker than wild type, and continue to thicken in basal regions. Nuclei are compact but similar to wild type and have prominent nucleoli. Endomembranes are disorganized (Fig. 1C) and putative Golgi equivalents, which occasionally resemble wild type in near-apical regions (not shown), become swollen and develop electron dense aggregates (Fig. 1D).

3.1. Cloning and molecular analysis of the hypA locus

hypA was mapped to chromosome IR (Kaminskyj and Hamer, 1998) and was cloned by complementing *hypA1* using the chromosome I specific cosmid library of Brody et al. (1991). Cosmid L22E6 generated dozens of transformants per microgram DNA. Complementing activity was subcloned to a 4.8-kb *Eco*RI fragment, pSKJ1 (Table 1). A 1.8-kb *Sac*I subclone of pSKJ1, pSKJ13, repaired the *hypA1* defect, indicating successful
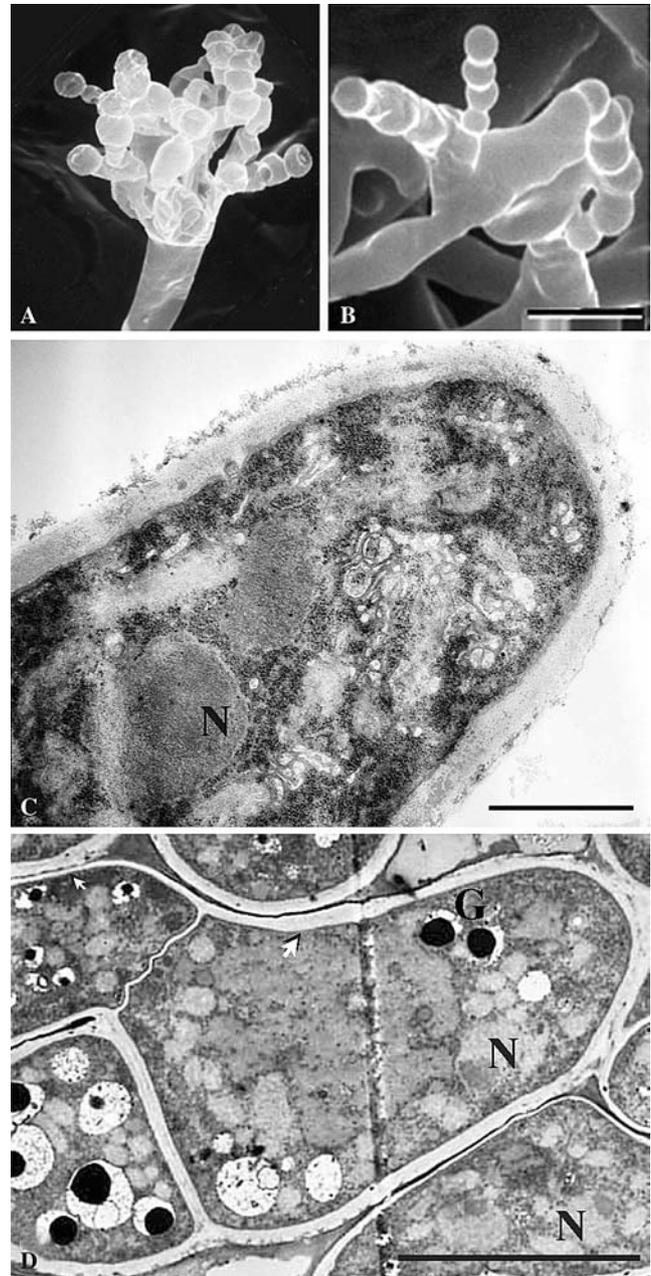

Fig. 1. Electron micrographs of *hypA1* (ASK30) and *hypA6* (ASH80) strains grown at 42 °C. Scanning electron micrographs of conidiophores and conidia of *hypA1* (A) and *hypA6* (B) strains. Transmission electron micrographs of near-median sections through *hypA1* cells grown for 14 h (C) and 5 days (D) at 42 °C. The hyphal walls produced by *hypA1* strains at 42 °C are at least fourfold thicker than those produced at 28 °C (not shown), which resemble wild type. Hyphal walls of *hypA1* strains produced at 42 °C continue to increase in thickness over time: walls of a relatively young branch in D are indicated by small arrows; older walls of the parent hypha are indicated by a large arrow. The septum at the base of the branch is abnormal. At 42 °C, the nuclei (N) of *hypA1* strains are compact but otherwise resemble wild type. In contrast, at 42 °C the *hypA1* Golgi equivalents (G) become swollen and contain electron dense aggregates, which typically are larger in older cells. Bar in $C = 1$ μm; bar in A, B, $D = 10$ μm.

cloning of *hypA*. The 3′-end of the *hypA*-coding region was isolated as a 2.8-kb *Cla*I fragment, pSKJ22, which overlaps pSKJ1 by 180 bp.

The *hypA* cDNA was cloned by 5′- and 3′-RACE (Shi and Kaminskyj, 2000; Shi et al., 2002). The *hypA* locus (GenBank AF001273 and AY251281) has CCAAT and TAAT motifs at −15 and −90 bases, respectively, with respect to the first ATG, suggesting that this is the translation start site. *hypA* encodes a predicted protein (HYPA) of 1474 amino acids with a weight of 161.9 kDa and a *pI* of 6.10. 3′-RACE revealed two polyadenylation sites, 271 and 331 bp, respectively, downstream from the stop codon. HYPA lacks a leader peptide, suggesting it is cytoplasmic, and also lacks signal sequences for nuclear localization, despite having a putative leucine zipper (beginning at leucine-664), residues to provide salt bridge stabilization for the resulting helix, and a potential bzip recognition sequence in the 5′-untranslated region. HYPA has numerous consensus phosphorylation sites for cAMP, cGMP, and tyrosine kinases.

hypA cDNA sequencing revealed two introns, 97 bp (beginning at cDNA position 151: CAATCGAAgtgagtt actcgaagacggaagaatgtcttttggattgcctgtagaaatgatgttgcaag ggaccgtttcgctgatttgcaattctcctaatattagACATGTTC) and 57 bp (beginning at cDNA position 1153: TTCAG GTTtgttatactttctactggagattgtttaagtgctaagaacttcctgtccat aggttCCTCCAAT), creating a single open reading frame of 4442 bp after transcript maturation. Neither of these introns conform to the AG-intron-G consensus described by Bhattacharya et al. (2000).

Southern blots of *A. nidulans* genomic DNA cut with seven restriction enzymes and probed with pSKJ13 recognized single bands; *Xho*I cuts pSKJ13 once and the pSKJ13 probe recognized two bands in *Xho*I-digested *A. nidulans* genomic DNA (not shown). Thus, *hypA* is a single copy gene. Northern blots probed with pSKJ1, pSKJ13 or internal amplicons recognized a single band at 5.4 kb.

Aspergillus nidulans hypA has full-length orthologs in filamentous fungi and yeasts, and has a 200 amino acid region with similarity to sequences in plants and ani-

mals. (Table 2; Fig. 2). By itself, this region has no homologies using BLAST analysis.

3.2. hypA is not an essential gene

hypA was replaced by *argB* (Fig. 3A) in the haploid *argB*-deletion strains A850 (Figs. 3B–E), and A851 (not shown), creating two types of arginine prototroph: slow-growing morphologically abnormal colonies and colonies which morphometry showed were statistically similar to wild type. We interpret these to be *hypA* deletion (Δ*hypA*) and *argB* ectopic insertion strains, respectively. Isolated haploid Δ*hypA* strains grew slowly on top of agar medium amended with 1 M sucrose. They did not grow on agar medium lacking osmoticum, nor into 1 M sucrose liquid medium. Occasionally, regions of Δ*hypA* hyphae were similar to wild type in width, but they developed frequent blebs (Figs. 3B and C). In basal regions these blebs often ruptured even in the absence of obvious physical disturbance. On 1 M sucrose agar, Δ*hypA* strains produced conidia after incubation for three weeks or more at 28 °C (Figs. 3D and E). The Δ*hypA* conidium diameter was up to double that of wild type, suggesting a loss of size control, and about one third were anucleate (Fig. 3E, and lower inset). Nevertheless. some Δ*hypA* conidia were viable at 28 °C. At least one conidium appeared to be germinating while still on the conidiophore (Fig. 3E upper inset). 28 °C-grown Δ*hypA* germlings arrested after upshift to 42 °C and became anucleate, and at 42 °C Δ*hypA* conidia did not germinate. In contrast, putative ectopic insertion strains grew well without osmoticum, and had wild-type hyphae and conidia. We were unable to harvest enough DNA from haploid Δ*hypA* germlings for Southern blot analysis, so we used PCR (Fig. 3F). With primers P9Xba and P14Kpn and *Taq* DNA polymerase, we amplified the expected 3.7 kb band using pΔ*hypA*::*argB* template, and using genomic DNA from two haploid deletion strains (Fig. 3F). However, *Taq* does not amplify long segments efficiently, and we were unable to visualize the expected 6.6 kb band from genomic DNA of A850. *Pfx* DNA

Table 2
Predicted gene products related to *Aspergillus nidulans* HYPA

	% identical	% positive	Region of similarity in *A nidulans* HYPA
Neurospora crassa	36	53	1–1474
Schizosaccharomyces pombe	24	40	1–1474
Candida albicans	21	38	1–1474
Saccharomyces cerevisiae	20	37	1–1474
Ashbya gossypii[a]	21	36	1–1474
Candida albicans[b]	20	37	1–1474
Arabidopsis thaliana	32	52	766–887
Oryza sativa	33	46	787–875
Drosophila melanogaster	22	38	782–1007
Caenorhabditis elegans	25	42	712–877

[a] T. Gaffney, Syngenta Agri Biotech Research Inc., *personal communication*.
[b] C. Bachewich, Biotechnology Research Centre, NRC, *personal communication*.

* hypA1 hypA6 G329R

Fig. 2. Alignment of *hypA* and fungal ortholog predicted peptides: *Aspergillus nidulans* (An), *Neurospora crassa* (Nc), *Schizosaccharomyces pombe* (Sp), and *Saccharomyces cerevisiae* (Sc), showing conserved (black boxes) and semi-conserved (grey boxes) amino acid residues.

polymerase can amplify long segments, but its proof-reading function results in primer degradation unless they are phosphorothioated (Skerra, 1992). We were able to amplify a 6.6-kb band from A850 gDNA using *Pfx* with P9Xba and P14Kpn (Fig. 3F) although there was evidence of primer degradation. We also amplified a strong 3.7 kb band from pΔ*hypA*::*argB*. Taken together, the haploid strains shown in Figs. 3B–E appear to be Δ*hypA*.
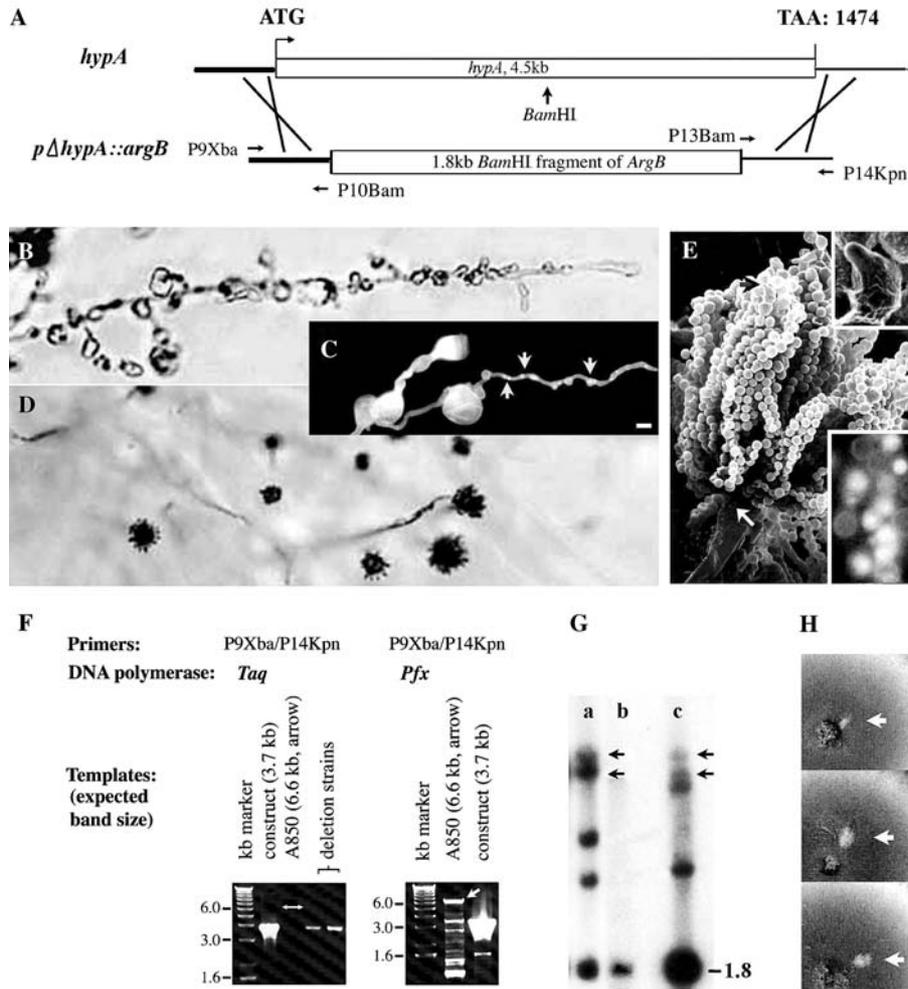
Fig. 3. *hypA* deletion. (A) Cartoon of *hypA* (not to scale), with the unique *Bam*HI site indicated by the arrow, and of the pΔ*hypA*::*argB* insert which was designed to replace *hypA* with *argB*. The primers were used to amplify flanking regions (shown as bars) and for PCR analysis of haploid Δ*hypA* strains. After transforming pΔ*hypA*::*argB* into the haploid Δ*argB* strain A850, arginine prototrophs were selected on MM containing 1 M sucrose. Δ*hypA* strains had weak growth (B–D), whereas ectopic *argB* integrants had wild-type growth (not shown). Transmitted light (B,D) and epifluorescence (C) micrographs of a haploid Δ*hypA* strain (bar represents 10 μm). (B) Δ*hypA* hyphae growing on 1 M sucrose agar, (C) stained with Hoechst 33258 (for nuclei, arrows) and Calcofluor (for walls), (D) Δ*hypA* strain beginning to conidiate after three weeks at 28 °C. (E) Scanning electron micrograph of a Δ*hypA* conidiophore after four weeks at 28 °C. Note variation in spore size. White arrow indicates the conidiophore vesicle. Black arrow and upper insert: germinating spore. Lower insert: Freshly harvested Δ*hypA* spores stained with Hoechst 33258, showing that some are anucleate. (F) PCR analysis of haploid Δ*hypA* strains using primers P9Xba/P14Kpn. *Taq* DNA polymerase was used to amplify pΔ*hypA*::*argB*, and genomic DNA from A850 and two deletion strains, identified on the basis of phenotype. This generated amplicons of 3.7 kb for pΔ*hypA*::*argB*, and 3.7 kb for the deletion strains. We expected a 6.6 kb amplicon for A850, but it was not efficiently amplified by *Taq*: this band position is represented by a double headed arrow. *Pfx* DNA polymerase was used to amplify A850 genomic DNA and pΔ*hypA*::*argB*, producing the expected 6.6 kb band (white arrow) and 3.7 kb band, respectively. These primers were not 3'phosphorothioated, so there are additional, smaller bands due to primer degradation from *Pfx* proofreading activity. (G) The diploid A852 strain was transformed with pΔ*hypA*::*argB*, creating arginine prototrophs, that were either *hypA*, Δ*argB*/Δ*hypA*::*argB*, or ectopic integrants. Southern analysis probed with pΔ*hypA*::*argB* of (a and c) *Bam*H1 digested genomic DNA of a *hypA*, Δ*argB*/Δ*hypA*::*argB* strains, (b) the 1.8 kb *argB* insert. The *hypA*-flanking bands recognized by the homologous arms are indicated by arrows in a and c. (H) The strain in (Ga) was treated with benomyl. Haploidizing *hypA*, Δ*argB*/Δ*hypA*::*argB* explants produced small areas with yellow conidia (arrows). Thus, the *hypA* deletion event depicted in Ga and H is on the chromosome copy that has *yA1*.

hypA was deleted in the diploid Δ*argB* strain A852, where we could confirm knockout of one copy of *hypA* by Southern blot. The A852 pΔ*hypA*::*argB* transformants were arginine prototrophs that did not require osmoticum to grow. *Bam*HI-digested genomic DNA from A852 and transformant strains had two bands >9 kb that were recognized by the homologous arms of

Δ*hypA*::*argB* (arrows in Figs. 3Ga and Gc). Transformant strains also had the 1.8-kb band corresponding to *argB* (cf. Fig. 3Gb). Transformants were treated with benomyl (Kaminskyj, 2001), after which haploidizing explants produced both yellow and green sectors. One homolog of chromosome I in the A852 diploid is marked with *yA1*; *hypA* and *yA* are about 18 map units

apart on chromosome IR. We were unable to isolate ΔhypA, argB haploid sectors, presumably because they were unable to grow fast enough to compete. We found tiny areas with yellow conidia (arrows in Fig. 3H) in explants from the haploidized colony shown in Fig. 3Ga. We interpret these yellow conidia as being produced by a ΔhypA nucleus, where the deletion was on the chromosome I copy with yA1. These conidia were impaired for germination and growth. Together, our data show that hypA is not essential, and that haploid ΔhypA strains are severely compromised compared to wild type.

3.3. Mutations causing hypA1 and hypA6

Genomic DNA samples from hypA1 and hypA6 strains, and A28 (the mutagenesis parent) were amplified by PCR, and sequenced. A single base pair mutation was identified in both hypA1 and hypA6 genomic DNA causing an amino acid substitution from glycine-329 to arginine-329, G329R. Corresponding DNA sequences are: hypA ggg: glycine, hypA1 and hypA6 agg: arginine. Because this mutation is found in the region encompassed by pSKJ13, which can repair hypA1, we tested whether it caused the hypA1 defect. We amplified this region from cosmid L22E6 and from A28 genomic DNA, and found that it was able to rescue the temperature sensitive phenotype in both hypA1 and hypA6 strains. In addition, both the hypA1 and hypA6 strains had two nonconservative amino acid substitutions, K885F and E932K with respect to the (unstated, likely A4) strain used by Brody et al. (1991) to generate the library containing cosmid L22E6 used in cloning hypA. These latter two nonconservative amino acid substitutions were also found in A28, and amplicons spanning these lesions from wild-type hypA template were not able to complement strains containing hypA1 or hypA6 alleles.

3.4. hypA roles in secretion efficiency and endomembrane arrays

Aspergillus nidulans hypA is related to S. cerevisiae TRS120, a regulatory component of the TRAPP II complex that mediates transit through the Golgi equivalent, an early stage in secretion. Given its close relationship to TRS120, we investigated the effect of hypA1 on secretion by comparing the ability of A. nidulans germlings to secrete amylase at 28 and 42 °C.

Wild type and hypA1 strains were grown on CM (which contains glucose), on MM containing 1% amylose as sole carbon source (MM-amylose), and on Difco nutrient agar containing 1% amylose (NA-amylose). Nutrient agar contains protein hydrolysates that can support A. nidulans growth without added carbohydrates. Amylase activity was assayed by flooding plates with 0.1% iodine in 1% KI (IKI): regions of

amylose degradation are seen as a yellow halo against dark blue.

At 28 °C, growth of hypA1 strains on MM-amylose resembled wild type (not shown). The hypA1 germlings arrested by 12–14 h on MM-amylose at 42 °C (Fig. 4A), with no evidence of amylose degradation. Only few of these germlings grew enough to deposit a septum at the spore to germ tube junction. This suggests hypA1 germlings are unable to secrete sufficient amylase at 42 °C to support growth beyond the stores in the conidium. In contrast, on CM at 42 °C, germlings typically were able to branch and deposit two or more septa (Fig. 4B). Germlings were able to grow for at least 24 h at 42 °C on NA (not shown) and on NA-amylose (Fig. 4C), and were able to branch and deposit multiple septa. In 24 h growth at 42 °C on NA-amylose, hypA1 cells had secreted enough amylase to create a narrow halo after IKI flooding (Fig. 4D). Thus, hypA1 strains have reduced amylase secretion at 42 °C.

We examined the endomembranes of wild type, hypA1 and hypA6 strains grown at 28 and 42 °C using the in vivo endomembrane dye FM4-64 (Fischer-Parton et al., 2000). At 28 °C, the endomembranes of wild type, hypA1 and hypA6 strains stain strongly in the central cytoplasm of near-apical regions, culminating in a Spitzenkörper (Fig. 5A). In contrast at 42 °C, while the endomembranes of wild-type strains resembled those at 28 °C (not shown), those of hypA1 and hypA6 strains

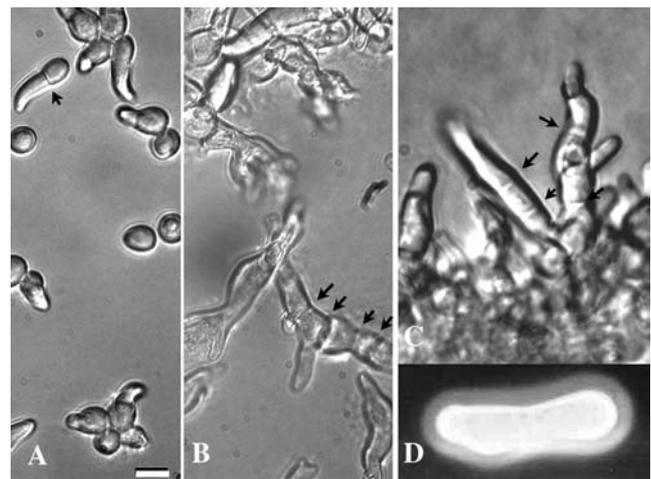Fig. 4. Growth of hypA1 cells on various carbon sources after 24 h at 42 °C. (A) On MM containing amylose as the sole carbon source, hypA1 germlings ceased growth at a stage equivalent to about 14 h on CM, which contains glucose. A few germlings were able to deposit a septum (arrow) at the spore to germ tube junction. (B) Growth of hypA1 germlings on CM shows branching and deposition of multiple septa (arrows). (C) Margin of a colony of hypA1 cells (shown in D) grown on nutrient agar plus 1% amylose, showing growth similar to that on CM (due to protein hydrolysates in the NA), including branching and multiple septa. (D) When this plate was flooded with iodine solution, the amylose near the colony had been degraded leaving a pale halo, whereas undegraded amylose further from the colony stained darkly. Bar for A–C = 10 μm.
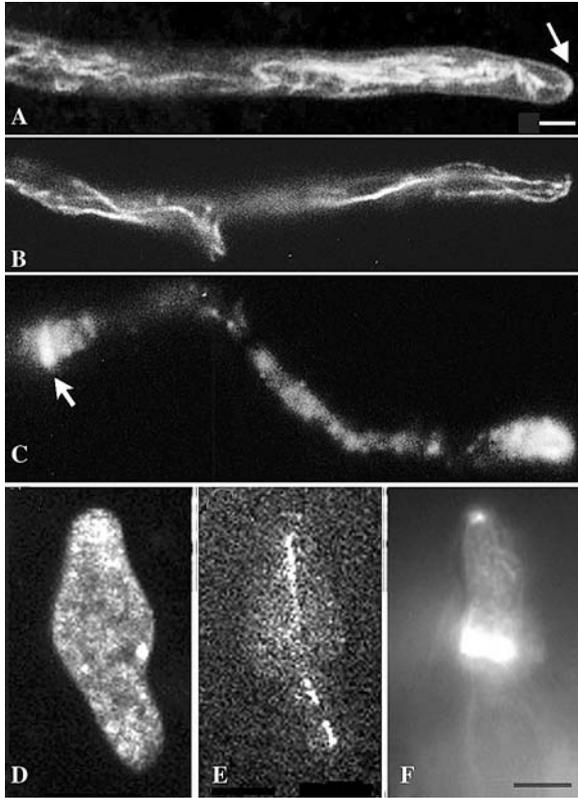
Fig. 5. Fluorescence images of endomembrane and cytoskeletal arrays of wild type (A–C) and *hypA1* (D–F) strains. (A) Confocal laser scanning image of FM4-64 stained endomembranes in wild-type *Aspergillus nidulans*. Arrow indicates the Spitzenkörper. Immunofluorescence images of cytoplasmic microtubules (B) and actin (C) in wild-type *A. nidulans*. The cytoplasmic microtubules follow the longitudinal axis of the cell. Cytoplasmic actin arrays are concentrated at the tip and at a developing septum (arrows), and are relatively less abundant in the near-apical cytoplasm. Bar for A–C = 2 μm. Confocal laser scanning images of a *hypA1* germling growing at 42 °C, showing (D) FM4-64 stained endomembranes, and (E) GFP-tagged cytoplasmic microtubules. Compared to wild type, at 42 °C the *hypA1* endomembranes are diffuse and lack an obvious Spitzenkörper, and the cytoplasmic microtubule population is reduced but has a normal distribution. (F) Immunofluorescence localization of actin in a *hypA1* germling grown at 42 °C and processed using freeze permeabilization. Actin is concentrated at the apex and at a developing septum. There are diffuse actin arrays in the near-apical cytoplasm. Bar for D–F = 5 μm.

were diffuse, and were only slightly more prominent near the tip (Fig. 5D). Wild-type endomembrane arrays and Spitzenkörper reformed in less than an hour after 42 °C-grown *hypA1* and *hypA6* cells were transferred to 28 °C, coincident with the formation of wild-type branches (Sha, 2003).

3.5. Effect of hypA mutations on cytoskeletal arrays

Aspergillus nidulans hyphae have polarized cytoplasmic microtubule (Han et al., 2001) and actin arrays (Harris et al., 1994). What are the effects of the

hypA1 and *hypA6* mutations on these arrays? Wild-type *A. nidulans* cytoplasmic microtubules collectively extend the length of the hyphae (Fig. 5B). The effect of 42 °C growth on cytoplasmic microtubules in *hypA1* strains was imaged with GFP-tagged α-tubulin. Few cytoplasmic microtubules were seen in *hypA1* strains grown at 42 °C, usually only one at any longitudinal position, but they retained normal positioning along the axis of the germling (Fig. 5E). Mitotic spindles were normal in appearance and kinetics (Sha, 2003), consistent with previous findings (Kaminskyj and Hamer, 1998).

Wild-type *A. nidulans* actin arrays in are concentrated at hyphal tips and at developing septa (Fig. 5C), a site of secondary wall deposition. Actin arrays *hypA1* germlings grown at 42 °C were diffuse in the apical cytoplasm, with a small area of concentration at the tip (arrow in Fig. 5F; this image was overexposed to highlight the apical arrays). The amount of actin in 42 °C-grown *hypA1* tips was substantially less than is typical in wild-type cells. Actin was also associated with developing septa (Fig. 5F).

4. Discussion

The *hypA* locus was identified from a morphological screen of temperature-sensitive *A. nidulans* mutant strains, mapped to chromosome IR (Kaminskyj and Hamer, 1998), and is represented by two temperature-sensitive alleles. *hypA1*, and *hypA6* (= *podA1*, Harris et al., 1999; = *swoE1*, Momany et al., 1999) strains have wild-type morphology at 28 °C, but at 42 °C they are slow-growing with aberrant hyphal profiles that continue to increase in width well behind the apical zone of expansion. The 42 °C phenotype of a *hypA1/hypA6* diploid is like that of *hypA1* (Kaminskyj and Hamer, 1998). *hypA1* and *hypA6* were originally assumed to be allelic rather than identical since they were generated in independent mutagenesis experiments and they are the only temperature sensitive *hypA* strains in 1809 isolates, the total in the Harris et al. (1994) and Kaminskyj and Hamer (1998) collections. It seemed unlikely that the same lesion would occur twice in a single large gene in a limited collection of strains. Nevertheless, *hypA1* and *hypA6* have identical coding sequences and collectively can be called *hypA1*. Like ASK30 and ASH80, the A28 strain has K885F and E932K non-conservative amino acid changes with respect to the strain used by Brody et al. (1991) to create the chromosome specific-cosmid library used to clone *hypA*. Neither of these latter residues is at a conserved position, and for each of these residues the *S. cerevisiae* ortholog has the alternate residue (F and K, respectively) at that position. With the *A. nidulans* genomic sequence now released, it should be useful to compare all *A. nidulans* gene sequences to identify

regions in other cloned genes where nonconservative changes do not have a functional consequence.

Differences in published reports on the phenotypes of *hypA1* (Kaminskyj and Hamer, 1998) and *hypA6* (=*podA1*; Harris et al., 1999) appear to have been due to numbers of cells examined, and possibly also to a difference in nutritional background of the strains originally analyzed. The ASH80 strain used by Harris et al. (1999) has *pabaA6* in its nutritional background, which causes a minor phenotypic anomaly at 28 °C: it results in yellow rather than green conidia on yeast extract-glucose-paba medium (Kaminskyj, 2001). We have not investigated the phenotypic effects of *pabaA6* at 42 °C. Morphometric comparison of ASK30 (*hypA1; pyroA4*), ASK39 (*hypA1, pabaA6*), and ASH80 (*hypA6, pabaA6*) showed statistical similarity for number of tips and septa produced at 42 °C, and for ability to form wild-type branches after growth at 42 °C followed by shifting to 28 °C (Sha, 2003).

Momany et al. (1999) suggested that *hypA* (=*swoE*) is required for hyphal morphogenesis but not for establishing or maintaining polarity. However, shifting 42 °C-grown *hypA1* germlings to 28 °C ("downshifting") causes initiation of wild-type branches beginning within an hour of downshift (Kaminskyj and Hamer, 1998; Sha, 2003). Branch formation requires localized wall softening to permit new cell extension. In *hypA1* strains after downshifting, the thick, restrictive-temperature *hypA1* walls are degraded (presumably by endoglucanases) in very restricted regions that subtend the wild-type branches (Kaminskyj and Boire, in preparation). This suggests that nascent areas capable of polarization, presumably involving HYPA, exist in 42 °C-grown cells with the *hypA1* and *hypA6* alleles and these can be activated by shifting to permissive temperature.

The G329R mutation is in a conserved region of HYPA. As a small and hydrophobic amino acid, this glycine is more likely to be buried in a folded polypeptide than is the larger, hydrophilic arginine. The region around HYPA residue 329 is predicted to have a β-sheet structure for both glycine-329 and arginine-329 forms, but this does not indicate whether the side chain is exposed. The arginine may be configurationally restricted at 28 °C compared to 42 °C, resulting in a conformational change that compromises HYPA functionality. A *hypA1, nimX3* double mutant has a permissive temperature phenotype (slow wild-type growth at 28 °C), whereas a *hypA1, nimX2* double mutant does not (Kaminskyj, 2000), suggesting at least one interaction that is likely to important for active tip cells *versus* quiescent basal cells that may involve *hypA*.

HYPA appears to be cytoplasmic, like TRS120, since it lacks a signal peptide and organelle localization signals, and putative transmembrane regions. The *hypA1* upshift phenotype is cell-type specific, suggesting that HYPA function could be regulated by differential phosphorylation in tip and basal cells, since it has consensus kinase phosphorylation sites.

Sacher et al. (1998) showed that *S. cerevisiae* TRS120p is a member of the cytoplasmic TRAPP (transport protein particle) complex involved in ER to Golgi equivalent transport. TRAPP I is required for tethering endoplasmic reticulum-derived coatomer vesicles to the *cis*-Golgi (Barrowman et al., 2000; Guo et al., 2000), whereas TRAPP II is implicated in Golgi equivalent trafficking through GTP exchange specificity (Wang and Ferro-Novick, 2002). TRS120p appears to be a regulatory component of TRAPP II, since overexpressing *TRS120* could not rescue the *bet3-1* secretion pathway growth defect (Sacher et al., 2000). *TRS120* has been shown to be essential, like the *Schizosaccharomyces pombe* (Dai, 2002) and the *Ashbya gossypii* (T. Gaffney personal communication) *hypA* orthologs, but unlike *A. nidulans hypA*. Reasons for this disparity are not yet clear, but correlate with *A. nidulans* alone amongst this group having a Spitzenkörper. Studying orthologs in other filamentous fungi may clarify this.

Temperature-sensitive mutants of *S. cerevisiae* TRAPP II components arrest with swollen Golgi equivalents (Sacher et al., 2001; Wang et al., 2000). At 42 °C, *A. nidulans hypA1* strains have at least some wild-type Golgi equivalents using transmission EM (Kaminskyj and Boire, in preparation), as well as many dilated vesicles with dark contents, particularly in older cells, which we interpret as aberrant Golgi equivalents. It is unclear whether these dilated vesicles retain function, but perhaps a limited number of recently-formed Golgi equivalents are sufficient to support slow growth.

In wild-type *A. nidulans*, endomembrane arrays visualized with FM4-64 are localized predominantly in the central cytoplasm and are much more abundant in near-apical than in basal cytoplasm. However in *hypA1* strains at 42 °C, endomembrane arrays stained with FM4-64 were diffuse and similar in abundance in peripheral versus central cytoplasm, and had only slightly greater abundance in apical regions. Consistent with this, transmission EM shows that *hypA1* strains grown at 42 °C have many areas of cytoplasm that appear to contain poorly organized endomembrane arrays (Figs. 1C and D). FM4-64 staining of *hypA1* strains grown at 42 °C also shows relatively brightly stained areas that may be the dilated vesicles discussed above. Also consistent with aberrant endomembrane system in *hypA1* cells grown at 42 °C, secretion of amylase was reduced to the extent that they could not survive on amylose as a sole carbon source.

Tip growth and secretion require actin and cytoplasmic microtubules for transport of exocytic vesicles. In *hypA1* cells grown at 42 °C, both actin and cytoplasmic microtubules were reduced in abundance. Nevertheless, they retained overall normal distributions, as

expected given the ability of *hypA1* cells to complete their asexual life cycle at 42 °C. Wild-type *A. nidulans* hyphae typically contain several long cytoplasmic microtubules as visualized by immunofluorescence (Fig. 5B), GFP-tagging (Han et al., 2001, Xiang et al., 2000), and transmission EM (Meyer et al., 1987). In contrast, *hypA1* strains grown at 42 °C have few cytoplasmic microtubules, consistent with their slow growth rate, but these have normal distribution along the longitudinal hyphal axis.

Bartnicki-Garcia (1973) proposed that hyphal growth required a "delicate balance" of wall deposition and wall softening, so that for example conidia could swell prior to germination, and walls at nascent branch points could be softened prior to branch extension. The 42 °C phenotype of *hypA1* mutants is of hyphae that increase substantially in width in subapical regions (Kaminskyj and Hamer, 1998). Using transmission electron microscopy, these cells have at least fourfold thicker walls than wild-type (Kaminskyj and Boire, in preparation), which evokes an ongoing need for wall softening. Thus, the *hypA1* 42 °C phenotype provides novel support for Bartnicki-Garcia (1973) model of hyphal morphogenesis.

In *hypA1* strains at 42 °C it appears that Spitzenkörper function may be delocalized, so that exocytosis in its absence might occur with low efficiency. Spitzenkörper are not reported to be required for conidial swelling. Even at 42 °C, *hypA1* strains maintain a low level of cell polarity (germlings become at least twice as long as they are wide) reflecting the low polarization of their endomembrane and cytoskeletal arrays, and Δ*hypA* strains produce polarized hyphae. After downshift, polarity is quickly reestablished at branch sites, where extremely localized changes in wall structure imply a focused delivery of wall softening enzymes (Kaminskyj and Boire, in preparation). This suggests that some polarized secretion machinery exists at 42 °C that is rapidly activated after shifting to 28 °C, and that HYPA function is critical to wild-type Spitzenkörper activity. An *A. nidulans* transport protein particle, if it exists, may be somewhat different from that in *S. cerevisiae*, related to the lethal *versus* nonlethal deletion phenotypes in fungi lacking or having a Spitzenkörper, respectively.

In summary, *A. nidulans hypA* is involved in hyphal morphogenesis, through an apparent role in regulating endomembrane traffic. The *hypA1* and *hypA6* mutations are identical, and have defects suggesting that HYPA may play an organizing role in Spitzenkörper activity. *hypA* deletion strains are viable but severely compromised for growth. *hypA* has closely related sequences in filamentous fungi and in yeasts, and more distantly related sequences in other eukaryotes. Investigations of these may lead to insights into eukaryote cell morphogenesis.

References

Adachi, K., Hamer, J.E., 1998. Divergent cAMP signaling pathways regulate growth and pathogenesis in the rice blast fungus *Magnaporthe grisea*. The Plant Cell 10, 1361–1373.

Altschul, S.F., Gish, W., Miller, W., Myers, E.W., Lipman, D.J., 1990. Basic local alignment search tool. J. Mol. Biol. 215, 403–410.

Bachewich, C.L., Heath, I.B., 1997. The cytoplasmic pH influences hyphal tip growth and cytoskeleton-related organization. Fung. Genet. Biol. 21, 76–91.

Barrowman, J., Sacher, M., Ferro-Novick, S., 2000. TRAPP stably associates with the Golgi equivalent and is required for vesicle docking. EMBO J. 19, 862–869.

Bartnicki-Garcia, S., 1973. Fundamental aspects of hyphal morphogenesis. In: Ashworth, J.M., Smith, J.E. (Eds.), Microbial Differentiation. Cambridge University Press, Cambridge, UK, pp. 245–267.

Bartnicki-Garcia, S., 1990. Role of vesicles in apical growth and a new mathematical model of hyphal morphogenesis. In: Heath, I.B. (Ed.), Tip Growth in Plant and Fungal Cells. Academic Press, San Diego, pp. 211–232.

Bartnicki-Garcia, S., 2003. Hyphal tip growth: outstanding questions. In: Osiewacz, H.D. (Ed.), Molecular Biology of Fungal Development. Marcel Dekker, New York, pp. 29–58.

Bartnicki-Garcia, S., Bartnicki, D.D., Gierz, G., Lopez-Franco, R., Bracker, C.E., 1995. Evidence that Spitzenkörper behavior determines the shape of a fungal hypha: a test of the hyphoid model. Exp. Mycol. 19, 153–159.

Bhattacharya, D., Lutzoni, F., Reeb, V., Simon, D., Nason, J., Fernandez, F., 2000. Widespread occurrence of spliceosomal introns in the rDNA genes of ascomycetes. Molec. Biol. Evol. 17, 1971–1984.

Blanchard, M.M., Taillon-Miller, P., Nowotny, P., Nowotny, V., 1993. PCR buffer optimization with uniform temperature regimen to facilitate automation. PCR Meth. Appl. 2, 234–240.

Borgia, P.T., Dodge, C.L., 1992. Characterization of *Aspergillus nidulans* mutants deficient in cell wall chitin or glucan. J. Bacteriol. 174, 377–383.

Borson, N.D., Salo, W.L., Drewes, L.R., 1992. A lock-docking oligo(dT) primer for 5′and 3′ RACE PCR. PCR Meth. Appl. 2, 144–148.

Brody, H., Griffith, J., Cuticchia, A.J., Arnold, J., Timberlake, W.E., 1991. Chromosome specific recombinant DNA libraries from the fungus *Aspergillus nidulans*. Nucleic Acids Res. 19, 3105–3109.

Bruno, K.S., Aramayo, R., Minke, P.F., Metzenburg, R.L., Plamann, M., 1996. Loss of growth polarity and mislocalization of septa in a

Neurospora mutant altered in the regulatory subunit of cAMP-dependent protein kinase. EMBO J. 15, 5772–5782.

Dai, Y., 2002. Study of *hypA* in *Aspergillus nidulans* by suppressor analysis and gene knockout of the *hypA* orthologue in *Schizosaccharomyces pombe*. M.Sc. Thesis, University of Saskatchewan.

Dayton, J.S., Means, A.R., 1996. Ca$^{(2+)}$/calmodulin-dependent kinase is essential for both growth and nuclear division in *Aspergillus nidulans*. Mol. Biol. Cell 7, 1511–1519.

Don, R.H., Cox, R.T., Wainwright, B.J., Baker, K., Mattick, J.S., 1991. Touchdown PCR to circumvent spurious priming during gene amplification. Nucleic Acids Res. 19, 4008.

Fischer-Parton, S., Parton, R.M., Hickey, P.C., Dijksterhuis, J., Atkinson, H.A., Read, N.D., 2000. Confocal microscopy of FM4-64 as a tool for analysing endocytosis and vesicle trafficking in living fungal hyphae. J. Microsc. 198, 246–259.

Frohman, M.A., Dush, M.K., Martin, G.R., 1988. Rapid production of full-length complimentary DNA from rare transcripts: amplification using a single gene-specific oligonucleotide primer. Proc. Natl. Acad. Sci. USA 85, 8998–9002.

Gale, C.A., Bendel, C.M., McClellan, M., Hauser, M., Becker, J., Hostetter, M., 1998. Linkage of adhesion, morphogenesis, and virulence in *Candida albicans*. Science 279, 1355–1358.

Gems, D., Johnstone, I.L., Clutterbuck, A.J., 1991. An autonomously replicating plasmid transforms *Aspergillus nidulans* at high frequency. Gene 98, 61–67.

Gooday, G.W., 1994. Cell walls. In: Gow, N.A.R., Gadd, G.M. (Eds.), The Growing Fungus. Chapman and Hall, London, pp. 43–62.

Guo, W., Sacher, M., Barrowman, J., Ferro-Novick, S., Novick, P., 2000. Protein complexes in transport vesicle targeting. Trends Cell Biol. 10, 251–255.

Han, G., Liu, B., Zhang, J., Zuo, W., Morris, N.R., Xiang, X., 2001. The *Aspergillus* cytoplasmic dynein heavy chain and NUDF localize to microtubule ends and effect microtubule dynamics. Curr. Biol. 11, 719–724.

Harris, S.D., Hofmann, A.F., Tedford, H.W., Lee, M.P., 1999. Identification and characterization of genes required for hyphal morphogenesis in the filamentous fungus *Aspergillus nidulans*. Genetics 151, 1015–1025.

Harris, S.D., Morrell, J.L., Hamer, J.E., 1994. Identification and characterization of *Aspergillus nidulans* mutants defective in cytokinesis. Genetics 136, 517–532.

Heath, I.B., 1990. The roles of actin in tip growth of fungi. Int. Rev. Cytol. 123, 95–127.

Hecker, K.H., Roux, K.H., 1996. High and low annealing temperatures increase both specificity and yield in touchdown and stepdown PCR. Biotechniques 20, 478–485.

Ichinomiya, M., Horiuchi, H., Ohta, A., 2002a. Different functions of the class I and class II *chitin synthase* genes, chsC and chsA, are revealed by repression of chsB expression in *Aspergillus nidulans*. Curr. Genet. 42, 51–58.

Ichinomiya, M., Motoyama, T., Fujiwara, M., Takagi, M., Horiuchi, H., Ohta, A., 2002b. Repression of chsB expression reveals the functional importance of class IV chitin synthase gene chsD in hyphal growth and conidiation of *Aspergillus nidulans*. Microbiol. Read. 148, 1335–1347.

Jackson, S.L., Heath, I.B., 1990a. Evidence that actin reinforces the extensible hyphal apex of the oomycete *Saprolegnia ferax*. Protoplasma 157, 144–153.

Jackson, S.L., Heath, I.B., 1990b. Visualization of actin arrays in growing hyphae of the fungus *Saprolegnia ferax*. Protoplasma 154, 66–70.

Jackson, S.L., Heath, I.B., 1993. Roles of calcium ions in hyphal tip growth. Microbiol. Rev. 57, 367–382.

Kafer, E., 1977. Meiotic and mitotic recombination in *Aspergillus* and its chromosomal aberrations. Adv. Genet. 19, 33–131.

Kaminskyj, S.G.W., 2000. Septum position is marked at the tip of *Aspergillus nidulans* hyphae. Fung. Genet. Biol. 31, 105–113.

Kaminskyj, S.G.W., 2001. Fundamentals of growth, storage, genetics and microscopy in *Aspergillus nidulans*. Fung. Genet. Newsl. 48, 25–31. Available from <www.fgsc.net>.

Kaminskyj, S.G.W., Hamer, J.E., 1998. *hyp* Loci control cell pattern formation in the vegetative mycelium of *Aspergillus nidulans*. Genetics 148, 669–680.

Kaminskyj, S.G.W., Heath, I.B., 1994. A comparison of techniques for localizing actin and tubulin in hyphae of *Saprolegnia ferax*. J. Histochem. Cytochem. 42, 523–530.

Kaminskyj, S.G.W., Heath, I.B., 1996. Studies on *Saprolegnia ferax* suggest the general importance of the cytoplasm in determining hyphal morphology. Mycologia 88, 20–37.

Lopez-Franco, R., Bartnicki-Garcia, S., Bracker, C.E., 1994. Pulsed growth of fungal hyphal tips. Proc. Natl. Acad. Sci. USA 91, 12228–12232.

Makoto, F.M., Ichinomiya, T., Motoyama, H., Horiuchi, A., Tagaki, M., 2000. Evidence that the *Aspergillus nidulans* class I and class II chitin synthase genes, *chsC* and *chsA*, share critical roles in hyphal wall integrity and conidiophore development. J. Biochem. Tokyo 127, 359–366.

Mayorga, M.E., Gold, S.E., 1999. A MAP kinase encoded by the *ubc3* gene of *Ustilago maydis* is required for filamentous growth and full virulence. Mol. Microbiol. 34, 485–497.

McGoldrick, C.A., Gruver, C., May, G.S., 1995. *myoA* of *Aspergillus nidulans* encodes an essential myosin I required for secretion and polarized growth. J. Cell Biol. 128, 577–587.

Meyer, S., Kaminskyj, S.G.W., Heath, I.B., 1987. Nuclear migration in a nud mutant of *Aspergillus nidulans* is inhibited in the presence of a quantitatively normal population of cytoplasmic microtubules. J. Cell Biol. 106, 773–778.

Miller, D.D., Lancelle, S.A., Hepler, P.K., 1996. Actin microfilaments do not form a dense meshwork in *Lilium longiflorum* pollen tube tips. Protoplasma 195, 123–132.

Momany, M.M., Hamer, J.E., 1997. The relationship of actin, microtubules, and crosswall synthesis during septation in *Aspergillus nidulans*. Cell Motil. Cytoskel. 38, 373–384.

Momany, M., Westfall, P.J., Abramowsky, G., 1999. *Aspergillus nidulans swo* mutants show defects in polarity establishment, polarity maintenance and hyphal morphogenesis. Genetics 151, 556–567.

Motoyama, T., Fujiwara, M., Kojima, N., Horuichi, H., Ohta, A., 1997. The *Aspergillus nidulans* genes chsA and chsD encode chitin synthases which have redundant functions in conidia formation. Mol. Gen. Genet. 253, 520–528.

Motoyama, T., Kojima, N., Horuichi, H., Ohta, A., Takagi, M., 1994. Isolation of a chitin synthase gene (*chsC*) of *Aspergillus nidulans*. Biosci. Biotech. Biochem. 58, 2254–2257.

Munro, C.A., Schofield, D.A., Gooday, G.W., Gow, N.A.R., 1998. Regulation of chitin synthesis during dimorphic growth of *Candida albicans*. Microbiol. Read. 144, 391–401.

Osherov, N., Mathew, J., May, G.S., 2000. Polarity-defective mutants of *Aspergillus nidulans*. Fung. Genet. Biol. 31, 181–188.

Osmani, S.A., May, G.S., Morris, N.R., 1987. Regulation of the mRNA levels of *nim* A, a gene required for the G2-M transition in *Aspergillus nidulans*. J. Cell Biol. 104, 1495–1504.

Raudaskoski, M., Rupes, I., Timonen, S., 1991. Immunofluorescent microscopy of the cytoskeleton in filamentous fungi after quick-freezing and low temperature fixation. Exp. Mycol. 15, 167–173.

Riquelme, M., Reynaga-Peña, C.G., Gierz, G., Bartnicki-Garcia, S., 1998. What determines growth direction in fungal hyphae? Fung. Genet. Biol. 24, 101–109.

Sacher, M., Barrowman, J., Schleitz, D., Yates III, J.R., Ferro-Novick, S., 2000. Identification and characterization of five new subunits of TRAPP. Eur. J. Cell Biol. 79, 71–80.

Sacher, M., Barrowman, J., Wang, W., Horecka, J., Zhang, Y., Pypaert, M., Ferro-Novick, S., 2001. TRAPP I implicated in the

specificity of tethering of ER-to-Golgi transport. Mol. Cell 7, 433–442.

Sacher, M., Jiang, Y., Barrowman, J., Scarpa, A., Burston, J., Zhang, L., Schieltz, D., Yates III, J.R., Abeliovich, H., Ferro-Novick, S., 1998. TRAPP, a highly conserved novel complex on the cis-Golgi that mediates vesicle docking and fusion. EMBO J. 17, 2494–2503.

Sambrook, J., Fritsch, E.F., Maniatis, T., 1989. Molecular Cloning: A Laboratory Manual, second ed. CSHL Press, Cold Spring Harbor, New York.

Seiler, S., Nargang, F.E., Steinberg, G., Schliwa, M., 1997. Kinesin is essential for cell morphogenesis and polarized secretion in Neurospora crassa. EMBO J. 126, 3025–3034.

Sha, Y., 2003. Molecular and confocal microscopic comparisons of wild-type and temperature sensitive alleles of the Aspergillus nidulans morphogenetic locus hyp A. M.Sc. Thesis, University of Saskatchewan.

Shi, X., Kaminskyj, S.G.W., 2000. Optimizing 5'-RACE by ribo G-tailing a general template-switching oligonucleotide. Biotechniques 29, 1192–1194.

Shi, X., Karkut, T., Chahmanhkah, M., Alting-Mees, M., Hemmingsen, S.M., Hegedus, D., 2002. RACEing across a bridging oligonucleotide (BO-5 RACE). Biotechniques 32, 480–482.

Shi, Z., Christian, D., Leung, H., 1998. Interactions between spore morphogenetic mutations affect cell types, sporulation, and pathogenesis in Magnaporthe grisea. Mol. Plant Microbe Interact. 11, 199–207.

Skerra, A., 1992. Phosphorothioate primers improve the amplification of DNA sequences by DNA polymerases with proofreading activity. Nucleic Acids Res. 20, 3551–3554.

Som, T., Kolaparthi, V.S., 1994. Developmental decisions in Aspergillus nidulans are modulated by Ras activity. Mol. Cell. Biol. 14, 5333–5348.

Sone, T., Griffiths, A.J.F., 1999. The frost gene of Neurospora crassa is an ortholog of yeast cdc1 and affects hyphal branching via manganese homeostasis. Fung. Genet. Biol. 28, 227–237.

Strathmann, M., Hamilton, B.A., Mayeda, C.A., Simon, M.I.E.M., Palazzolo, M.J., 1991. Transposon-facilitated DNA sequencing. Proc. Natl Acad. Sci. USA 88, 1247–1250.

Wang, W., Sacher, M., Ferro-Novick, S., 2000. TRAPP stimulates guanine nucleotide exchange on Ypt1p. J. Cell Biol. 151, 289–295.

Wang, W., Ferro-Novick, S., 2002. A Ypt32p exchange factor is a putative effector of Ypt1p. Mol. Biol. Cell 13, 3336–3343.

Westfall, P.J., Momany, M., 2002. Aspergillus nidulans septin AspB plays pre- and postmitotic roles in septum, branch, and conidiophore development. Mol. Biol. Cell. 13, 110–118.

Whittaker, S.L., Lunness, P., Milward, K.J., Doonan, J.H., Assinder, S.J., 1999. sod^{VI}C is an alpha-COP-related gene which is essential for establishing and maintaining polarized growth in Aspergillus nidulans. Fung. Genet. Biol. 26, 236–252.

Wu, Q., Sandrock, T.M., Turgeon, B.G., Yoder, O.C., Wirsel, S.G., Aist, J.R., 1998. A fungal kinesin required for organelle motility, hyphal growth, and morphogenesis. Mol. Biol. Cell 9, 89–101.

Wybranietz, W.A., Lauer, U., 1998. Distinct combination of purification methods dramatically improves cohesive-end subcloning of PCR products. Biotechniques 24, 578–580.

Xiang, X., Han, G., Winkelmann, D.A., Zuo, W., Morris, N.R., 2000. Dynamics of cytoplasmic dynein in living cells and the effect of a mutation in the dynactin complex actin related protein Arp1. Curr. Biol. 10, 603–606.

Yelton, M.M., Hamer, J.E., Timberlake, W.E., 1984. Transformation of Aspergillus nidulans by using a trpC plasmid. Proc. Natl. Acad. Sci. USA 80, 1470–1474.